Three-Dimensional Structure of Neuropeptide K Bound to Dodecylphosphocholine Micelles†

Anjali Dike and Sudha M. Cowsik*

School of Life Sciences, Jawaharlal Nehru University, New Delhi 110067, India

Received November 8, 2005; Revised Manuscript Received January 7, 2006

ABSTRACT: Neuropeptide K (NPK), an N-terminally extended form of neurokinin A (NKA), represents the most potent and longest lasting vasodepressor and cardiomodulatory tachykinin reported thus far. NPK has been shown to have high selectivity for the NK2 receptor. Because the micelle-associated structure may be relevant to the NPK−receptor interaction, the three-dimensional structure of the NPK in aqueous and micellar environments has been studied by two-dimensional proton nuclear magnetic resonance (2D ^{1}H NMR spectroscopy) and distance geometry calculations. Proton NMR assignments have been carried out with the aid of correlation spectroscopy (DQF-COSY and TOCSY) and nuclear Overhauser effect spectroscopy (NOESY and ROESY) experiments. The interproton distances and dihedral angle constraints obtained from the NMR data have been used in torsion angle dynamics algorithm for NMR applications (DYANA) to generate a family of structures, which have been refined using restrained energy minimization and dynamics. The results show that in an aqueous environment NPK lacks a definite secondary structure, although some turn-like elements are present in the N terminus. The structure is well-defined in the presence of dodecylphosphocholine micelles. The global fold of NPK bound to DPC micelles consists of two well-defined helices from residues 9 to 18 and residues 27 to 33 connected by a noncanonical β turn. The N terminus of the peptide is characterized by a 3_{10} helix or a series of dynamic β turns. The conformational range of the peptide revealed by NMR and circular dichroism (CD) studies has been analyzed in terms of characteristic secondary features. The observed conformational features have been further compared to a NKA and neuropeptide γ (NPγ) potent endogenous agonist for the NK2 receptor.

Neuropeptide K (NPK),[1] a 36 amino acid residue, tachykinin peptide, with neurokinin A (NKA) at its C terminus, has been isolated from porcine brain (*1*) and regarded as a specific post-translational product of the PPT-A gene. The processing of this gene is tissue-specific and permits the preferential production of multiple products, including substance P (SP), NKA, NKA(3−10), neuropeptide γ (NPγ), and NPK. Next to SP, NPK is the major tachykinin in the cerebral cortex and hippocampus.

NKA, HKTDSFVGLM-NH_2

NPγ, DAGHGQISHKRHKTDSFVGLM-NH_2

NPK, DADSSIEKQVALLKALYGHGQISH-KRHKTDSFVGLM-NH_2

Several studies indicate that NPK represents thus far the most potent and longest lasting vasodepressor and cardiomodulatory tachykinin, whose actions appear to be mediated by a direct action on blood vessels and the autonomic nervous system, respectively (*2*). NPK is involved in contracting the gall bladder, causing protein extravasation, hypotension, and bronchial smooth muscle spasms (*3*). An important role of NPK in the nerve terminal region is to provide a pool or reservoir of the peptide precursor, which may be transformed readily into NKA when activity demands it (*4*). A comparison of the primary structure of NPK from bovine, human, porcine, and rat species reveals a striking sequence homology of 97−100% (*5*). Moreover, NPK was found more potent and more efficacious than SP as a stimulator of phosphatidylinositol turnover in the adult rat spinal cord; the high potency of NPK did not appear to be entirely attributable to the metabolic stability of the peptide (*6*). NPK is also more potent than SP as a sialogogue in the rat (*5*) and as a bronchoconstrictor in the guinea pig in vivo (*7*).

Three distinct G-protein coupled receptor subtypes NK1, NK2, and NK3 have been identified and cloned for tachykinins (*8*−*10*). The three receptors share a significant sequence similarity, interact differentially with the tachykinin peptides, and are uniquely distributed throughout the nervous system. While SP has a higher affinity for the NK1 type, NKA and NKB are thus far the endogenous ligands that exhibit the highest affinity for the NK2 and NK3 binding sites, respectively. NPK has been shown to have a higher selectivity for the NK2 receptor than NKA (*11*). The broad spectrum of action of NPK, which can be attributed to its increased size, more metabolic stability as compared to smaller tachykinins, and its improved selectivity for the NK2

† This work is supported through a grant from the Department of Science and Technology (DST), Government of India.

* To whom correspondence should be addressed. Telephone: 91-11-26177359 and 91-11-26170016. Fax: 91-11-26165886 and 91-11-26187338. E-mail: scowsik@yahoo.com.

[1] Abbreviations: NPK, neuropeptide K; NPγ, neuropeptide γ; NKA, neurokinin A; SP, substance P; DPC, dodecylphosphocholine; DQF-COSY, double-quantum-filtered correlation spectroscopy; NOESY, nuclear Overhauser enhancement and exchange spectroscopy; TOCSY, total correlation spectroscopy; NK, neurokinin.

10.1021/bi052287o CCC: $33.50
Published on Web 02/07/2006

receptor makes it a valuable tool for further research on tachykinin receptors.

Bioactive conformation of tachykinins have been extensively investigated using high-resolution nuclear magnetic resonance (NMR), circular dichroism (CD), and infrared (IR) spectroscopy. Solution structure for SP, NKA, NKB, physalaemin, eledoisin, and various naturally derived or synthetic analogues have been reported in various membrane mimetic solvents (*12*−*23*). The only NMR study reported for NPK is in 28% 2,2,2-trifluoroethanol (TFE), and it shows that NPK adopts a well-defined amphipathic α helix in its N-terminal half and is relatively disordered in its C-terminal half (*16*). Until now, there has been no report on the CD spectroscopic investigation of NPK as well as its three-dimensional structure in the micelle-bound form.

Several studies have suggested that the target cell surface influences receptor selection of peptides such as tachykinins through the accumulation of the ligand at the cell membrane, the induction of a specific conformation, and the orientation of the peptide (*24*−*28*). Although micelles are not a perfect mimetics of lipid bilayers, a substantial number of structural studies on peptides and proteins bound to micelles have indicated that valuable structural information can be obtained from NMR studies of such systems (*29*−*32*). Micellar systems have been used extensively in high-resolution NMR studies of the peptide−membrane interaction as membrane mimics (*33*−*36*). The dodecylphosphocholine (DPC) micelle is one of the most widely used membrane mimics for such studies (*35*). High-resolution NMR spectra can be obtained on peptides bound to micelles of perdeuterated lipids, taking advantage of the effective isotropic reorientation of the micelle-bound peptides.

We report here a three-dimensional structure of NPK in DPC micelles, one of the well-characterized model membrane systems. The structure has been deposited in the Protein Data Bank, and the PDB ID code is 2B19. This structure represents the first three-dimensional structure of NPK bound to DPC micelles. Several homonuclear two-dimensional NMR techniques (*37*), such as total correlation spectroscopy (TOCSY), double-quantum-filtered correlation spectroscopy (DQF-COSY), rotating frame Overhauser effect spectroscopy (ROESY), and nuclear Overhauser effect spectroscopy (NOESY), have been used in deriving the complete proton resonance assignments for NPK, in water and in the lipid medium. The NOESY cross-peak volumes have further been used to determine the interproton distances in three-dimensional space. An ensemble of model conformations has been generated for NPK in the lipid medium using DYANA (*38*). Also, the conformational features of NPK in aqueous and perdeuterated DPC micelles have been described and compared. CD spectroscopy has been used to explore various secondary-structural features of NPK in the presence of calcium ions and in different membrane mimetic environments, including TFE, TFE/water mixtures, sodium dodecyl sulfate (SDS), and DPC micelles. CD studies corroborate our NMR data. The structure of NPK is further compared with NKA and NPγ, which are potent endogenous NK2 receptor agonists in mammals.

MATERIALS AND METHODS

NPK (DADSSIEKQVALLKALYGHGQISHKRHKTDSFVGLM-NH_2) was custom-synthesized by Princeton Biomolecules (PA). The purity of the peptide reported by HPLC analysis was >98%. Perdeuterated DPC (d_{38}) was obtained from Cambridge Isotope Laboratories (MA).

CD Spectroscopy. CD spectra were recorded in a 0.1 cm cuvette on a Jasco, J-720 spectropolarimeter from 190 to 250 nm with 4 scans for all of the experiments. The instrument had been calibrated previously for wavelength using benzene vapor and for optical rotation using Camphorsulfonic acid-d_{10}. All of the experiments were carried out at room temperature. The bandwidth was 1 nm, and the scan speed was 50 nm/min. The peptide concentration was typically 33.5 μM in DPC, sodium phosphate buffer at pH 7.2, various ratios of the TFE/water mixture, and SDS micelles. For Ca^{2+} titrations, aliquots of stock solution of $CaCl_2$ in TFE solutions were added to the peptide solution to get the molar ratio of 1:1, 2:1, or 10:1. Prior to the calculation of the final ellipticity, all spectra were corrected by subtracting the spectra of respective solutions. CD intensity is expressed in terms of molar ellipticity [(θ) expressed in degrees cm^2 $dmol^{-1}$] according to the following equation:

$$[\theta] = \theta_{mdeg}/lC$$

where θ_{mdeg} is the measured ellipticity in millidegrees, l is the cell path length in centimeters, and C is the molar concentration of the protein or peptide.

Quantitative estimations of the secondary-structure contents from the CD spectra were made using CONTINLL software (*39*). Results reported are from 42 proteins data set. Other reference protein sets, such as 29, 37, 43, and 48, were also tested and gave rise to comparable results. The CD data analyzed by CONTINLL software are in good agreement with the values of two parameters R1 and R2, which are independent of inaccuracies in the determined peptide concentration, as well as those caused by small shifts in the wavelength (*36*). R1 is the ratio of the intensity of the maximum between 190 and 195 nm and the intensity of the minimum between 200 and 210 nm, and R2 is the ratio of the intensity of the minimum near 222 nm and the intensity of the minimum between 200 and 210 nm. For a random structure, R1 is positive and R2 is close to 0. On the other hand, in a highly helical state, R1 will be close to −2 and R2 will approach 1 (*31*, *40*).

NMR Spectroscopy. The NMR samples were prepared by dissolving 4.7 mg of NPK in approximately 0.5 mL of water (90% H_2O and 10% D_2O at pH 3.5). To investigate the conformation of NPK in a membrane-mimicking environment, an identical peptide sample was prepared to which 29 mg of perdeuterated DPC was added yielding in solution a lipid concentration of 146 mM. The lipid/peptide ratio of the NMR sample was 60:1. All 2D spectra were acquired in the phase-sensitive mode using a time-proportional phase incrementation (TPPI) method (*41*) at 300 K for water and 305 K for DPC micelles on a Bruker DRX 500 MHz NMR spectrometer. The homonuclear TOCSY (100 ms), NOESY (100, 150, 200, and 250 ms), DQF-COSY (80 ms), and ROESY (200 ms) were recorded with 64 scans, a relaxation delay of 1.5 s, a spectral width of 5020 Hz in both dimensions, 512 increments in t1, and 2000 data points in t2. The data were processed by XWINNMR software on Silicon graphics Fuel workstation (SGI, CA).

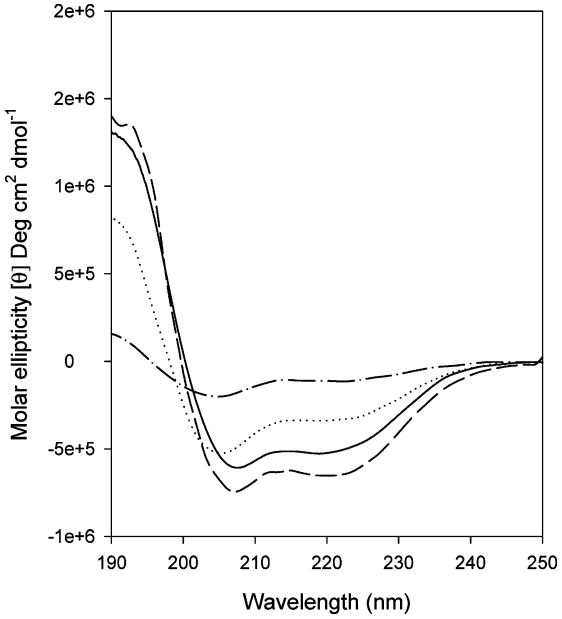

FIGURE 1: CD spectra of NPK: buffer (-·-), SDS micelles (···), 60% TFE (—), and DPC micelles (- - -).

NMR Restraints and Structure Calculation. The three-dimensional structure for NPK in DPC micelles was calculated using DYANA (*38*). All of the NOESY peak volumes on the 150 ms NOESY spectra were converted into distance constraints and divided into three classes: strong, medium ,and weak, with the distance ranges of 1.8−2.7, 1.8−3.5, and 1.8−5 Å, respectively. A total of 344 NOE distance constraints (154 intraresidue, 101 *i*, *i* + 1; 54 *i*, *i* + 2; 28 *i*, *i* + 3; and 7 *i*, *i* + 4) were calculated and used as input for DYANA. $^3J_{HN\alpha}$-coupling constants were obtained from high-resolution 1D spectrum, converted to dihedral angles by applying the Karplus relationship (*42*), and used as additional constraints for DYANA. A total of 50 structures were generated, of which 20 were selected on the basis of low target function values (≈1 Å) and subjected to restrained energy minimization.

RESULTS

CD Studies. Figure 1 shows that NPK lacks a definite secondary structure in an aqueous environment. In contrast, an α-helical structure is induced in different membrane mimetic environments such as 90% TFE, SDS micelles (64 mM), and DPC micelles (150 mM). All spectra have a minimum at 222 nm (helical nπ* transition) and a second minimum between 202 and 208 nm (overlapping helical and random-coil $\pi\pi$* transitions at 208 and 200 nm, respectively) (*43*−*45*). The presence of a single isodichroic point at 200 and 198.20 nm in TFE and SDS titrations, respectively (data not shown), indicates a two-state transition process between random-coil and helical structures. Secondary-structural features obtained are summarized in Table 1. The CD results indicate that NPK associates with TFE, SDS, and DPC micelles undergoing a conformational transition from a prevalently random-coil state (in buffer) to an α-helical state in the presence of micelles.

As shown in Figure 2, there is an increase in the helical content upon addition of Ca^{2+}. The data indicate the role of calcium in imparting conformational restraints on the peptide.

Table 1: Secondary-Structural Analysis of the NPK in Various Membrane Mimetic Environments Using CONTINLL with a 42-Reference Protein Set[a]

	secondary structure (%)						
environment	helix	strand	turn	unrd	rmsd	R1[b]	R2[b]
phosphate buffer at pH 7.2	7.7	31.9	15.5	45	0.054	−0.80	0.66
90% TFE	49.8	9.5	12.7	27.9	0.118	−1.77	0.82
DPC	58.1	3.9	13.8	24.2	0.038	−1.90	0.88
64 mM SDS	37.9	12.7	19.4	30.1	0.126	−1.73	0.69

[a] For convenience of data interpretation, we added the distorted and regular components of both helical and strand secondary-structural elements together to obtain the overall helical and strand structures in both Tables 1 and 2. [b] Here, R1 is the ratio of the intensity of the maximum between 190 and 195 nm and the intensity of the minimum between 200 and 210 nm, and R2 is the ratio of the intensity of the minimum near 222 nm and the intensity of the minimum between 200 and 210 nm.

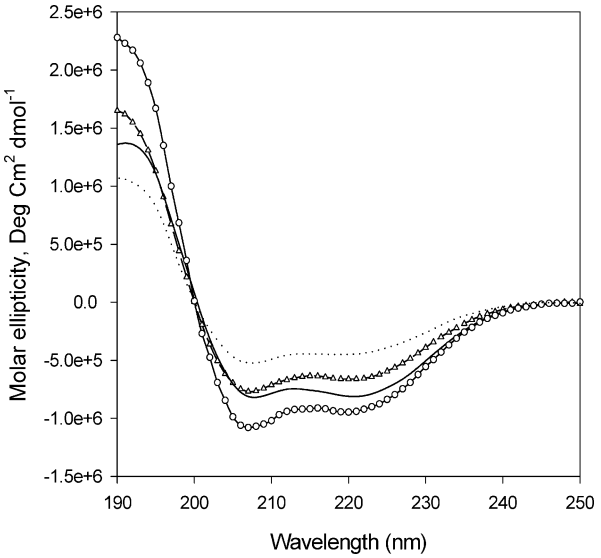

FIGURE 2: CD spectra of calcium titration of NPK. Different spectra in the figure represent various ratios of calcium/peptide: 100% TFE (···); 1:1 (△); 2:1 (—), and 10:1 (○), respectively.

Table 2: Effect of the Calcium Concentration on the Conformation of NPK Using CONTINLL with a 42-Reference Protein Set

environment (calcium/peptide ratio)	secondary structure (%)						
	helix	strand	turn	unrd	rmsd	R1[a]	R2[a]
100% TFE	52.1	8.5	10.7	28.6	0.060	−2.04	0.84
1:1	58.1	4.1	10	27.8	0.021	−2.14	0.85
2:1	60.8	2.2	10.9	26.2	0.017	−1.67	0.98
10:1	76.8	1.5	3.1	18.6	0.021	−2.11	0.85

[a] Here, R1 is the ratio of the intensity of the maximum between 190 and 195 nm and the intensity of the minimum between 200 and 210 nm, and R2 is the ratio of the intensity of the minimum near 222 nm and the intensity of the minimum between 200 and 210 nm.

Secondary-structural features obtained are summarized in Table 2.

NMR Studies. Preliminary 1D and 2D spectra of NPK were recorded in aqueous solution at various temperatures and were assigned completely. Another series of 1D and 2D proton NMR spectra were recorded for NPK in DPC micelles at 500 MHz. There were severe overlaps in the spectra. A great deal of effort was put into obtaining optimum pH and temperature to overcome problems because of overlap. The

structural stabilization was apparent in the NMR spectra upon addition of 20 mg or more of DPC-d_{38}. All subsequent experiments were performed under these solution conditions (DPC concentration of 146 mM) at 305 K.

Resonance Assignment and Secondary Shifts. Proton assignments were made by following standard sequence-specific assignment methods developed by Wüthrich (*37*). The entire spin systems of individual amino acid residues were identified through DQF-COSY and TOCSY experiments. The single Arg and Thr residues were easily assigned, but four leucines had a strong overlap. Lys14 was particularly difficult to assign from TOCSY but could be identified with the help of DQF-COSY and NOESY spectra. The ambiguities were completely resolved by a direct comparison of the fingerprint region of TOCSY and NOESY spectra. Complete sequential assignment of the spin systems was based on amide $d_{NN}(i, i + 1)$ cross-peaks and confirmed by H^{α}/amide $d_{\alpha N}(i, i + 1)$ as well as side-chain/amide $d_{\beta N}(i, i + 1)$ connectivities in a NOESY spectrum (parts a and b of Figure 3).

A similar assignment strategy was used for NPK in an aqueous environment (water). Because of the increased tumbling rate of the peptide in an aqueous environment, ROESY showed better results than NOESY. Therefore, the assignments were made by a direct comparison of TOCSY and ROESY spectra (parts a and b of Figure 4). Unlike DPC micelles, all of the spin systems were very well-resolved in water. Complete proton resonance assignments for NPK in the presence of membrane mimetic solvent (DPC) and in aqueous medium, thus obtained, are given as Tables 3 and 4 in the Supporting Information.

Analysis of Chemical-Shift Values. $C_{H\alpha}$ resonances are strongly dependent upon the local secondary structure. A simple method of Wishart and co-workers (*46*) has been adopted for predicting the secondary structure of proteins based on changes in their αH proton chemical shifts. Upfield shifts at least for three consecutive residues, relative to the random-coil values, are generally found for regions implicated in an α helix, and downfield shifts are generally found for those in β sheets. In DPC micelles, the secondary shift values (~ -0.1) observed from residues 1 to 18 and 28 to 36 suggest an ordered secondary structure in this region (Figure 5), consistent with the CD and NMR data on the existence of turn and helical conformation.

The percentage of bound conformers compared to the free conformers may be obtained by the determination of the amount of α helix observed. A semiquantitative estimation of the helical content of NPK when going from water to DPC micelles may be obtained from the average upfield shifts of the αH protons. In this procedure, the upfield shifts of αH protons of the region assumed to be helical are added together and averaged. The averaged upfield shifts are divided by 0.35 (0.35 ppm is assumed to correspond to 100% α helix), yielding a percentage of α helix (*31*). The semiquantitative estimate of helical content for residues 9−18 and 27−33 for NPK in DPC micelles thus calculated is 69.43%.

Interresidue NOEs and Secondary Structure. A summary of interresidue sequential and medium-range NOEs, which are important to characterize the secondary structure of NPK in DPC micelles and aqueous environment, is given in parts a and b of Figure 6, respectively. In the micellar environment, the intraresidue cross-peaks are more intense from residues 2 to 18 of NPK, thus indicating the stretch of the folded structure. Medium-range NOE connectivities, 6 $d_{NN}(i, i + 2)$, 10 $d_{\alpha N}(i, i + 2)$, 9 $d_{\alpha N}(i, i + 3)$, 5 $d_{\alpha\beta}(i, i + 3)$, along with 6 $d_{\alpha N}(i, i + 4)$ suggest the presence of an α helix in the region from residues 9 to 18. All measurable $3J_{NH\alpha}$-coupling constants for these residues are in the range of 3−6 Hz, further supporting a helix in this region.

A dense grouping of NOEs, 5 $d_{\alpha N}(i, i + 3)$, 6 $d_{\alpha N}(i, i + 2)$, 1 $d_{\alpha N}(i, i + 4)$, 7 sequential d_{NN} NOEs, and 4 $d_{NN}(i, i + 2)$ NOEs support the presence of a helix in the C terminus involving residues 27−33. On the other hand, the presence of 3 $d_{\alpha N}(i, i + 2)$, 2 $d_{NN}(i, i + 2)$, and a single $d_{\alpha N}(i, i + 3)$ between residues 34−36 suggests unwinding of the helix and fraying of the helix at the C terminus. A propensity of type II′β turn in the region from residues 19 to 26 can be inferred from the observation of several medium-range NOEs: $d_{\alpha N}(i, i + 2)$ (Gly18−Gly20, His19−Gln21, Gly20−Ile22, Gln21−Ser23, Ser23−Lys25, and His24−Arg26) and $d_{\alpha N}(i, i + 3)$ (Gly18−Gln21, Gly20−Ser23, Gln21−His24, and Ile22−Lys25). This is further supported by the $3J_{NH\alpha}$-coupling constants (>6 Hz) in this region. Toward the N terminus of the peptide, there are cross-peaks characteristic of a β turn or a 3_{10} helix. The observation of several $d_{\alpha N}(i, i + 3)$ NOEs (Ser4−Glu7, Ser5−Lys8, and Glu7-Val10) coupled with $d_{\alpha N}(i, i + 2)$ cross-peaks (Asp1−Asp3, Ala2−Ser4, Asp3−Ser5, Ser4−Ile6, Ser5−Glu7, Ile6−Lys8, and Glu7−Gln9) suggests partial unfolding via 3_{10} helix or turn-like elements in rapid equilibrium. Although identification of turns is less reliable than for regular secondary structures, the possibility of a β turn seems more pronounced in this region from residues 2 to 9, as seen by the absence of $d_{\alpha\beta}(i, i + 3)$ cross-peaks characteristic of 3_{10} helices (*47*).

In an aqueous environment, there are a few medium-range connectivities (2 $d_{NN}(i, i + 2)$, 4 $d_{\alpha N}(i, i + 2)$, and 1 $d_{\alpha N}(i, i + 3)$) in the region from residues 2 to 18. The remainder of the molecule displays many sequential NOEs, with some $(i, i + 2)$ contacts, but little further evidence of defined secondary conformation. Similarly, some turn-like elements are present toward the C terminus as seen by the presence of 1 $d_{NN}(i, i + 2)$ and 4 $d_{\alpha N}(i, i + 2)$ NOE connectivities. The presence of very few medium-range NOEs and absence of $d_{\alpha\beta}(i, i + 3)$ along with $d_{\alpha N}(i, i + 4)$ NOEs strongly suggests a lack of definite secondary structure of NPK in the aqueous environment. The structure in aqueous medium can be best described as a series of turns in dynamic equilibrium, and hence, no further calculation was done for the structure in water.

Three-Dimensional Structure Calculations. Different mixing times of NOESY spectra were used to evaluate the linear build-up of NOEs. Cross-peaks from a NOESY spectrum with a mixing time of 150 ms, which lies within the initial build-up of the NOE curve, were measured and divided into three classes. NOEs were classified into strong, medium, and weak NOEs according to their intensities and were converted into corresponding upper-bound interproton distance restraints of 2.7, 3.5, and 5.0 Å, respectively.

The three-dimensional structure of NPK in DPC micelles was determined using torsion angle dynamics algorithm for NMR applications, DYANA (*38*). A total of 385 distance constraints and angle constraints (from measured coupling constants, $^3J_{HN\alpha}$) were used as an input for DYANA. Initially,

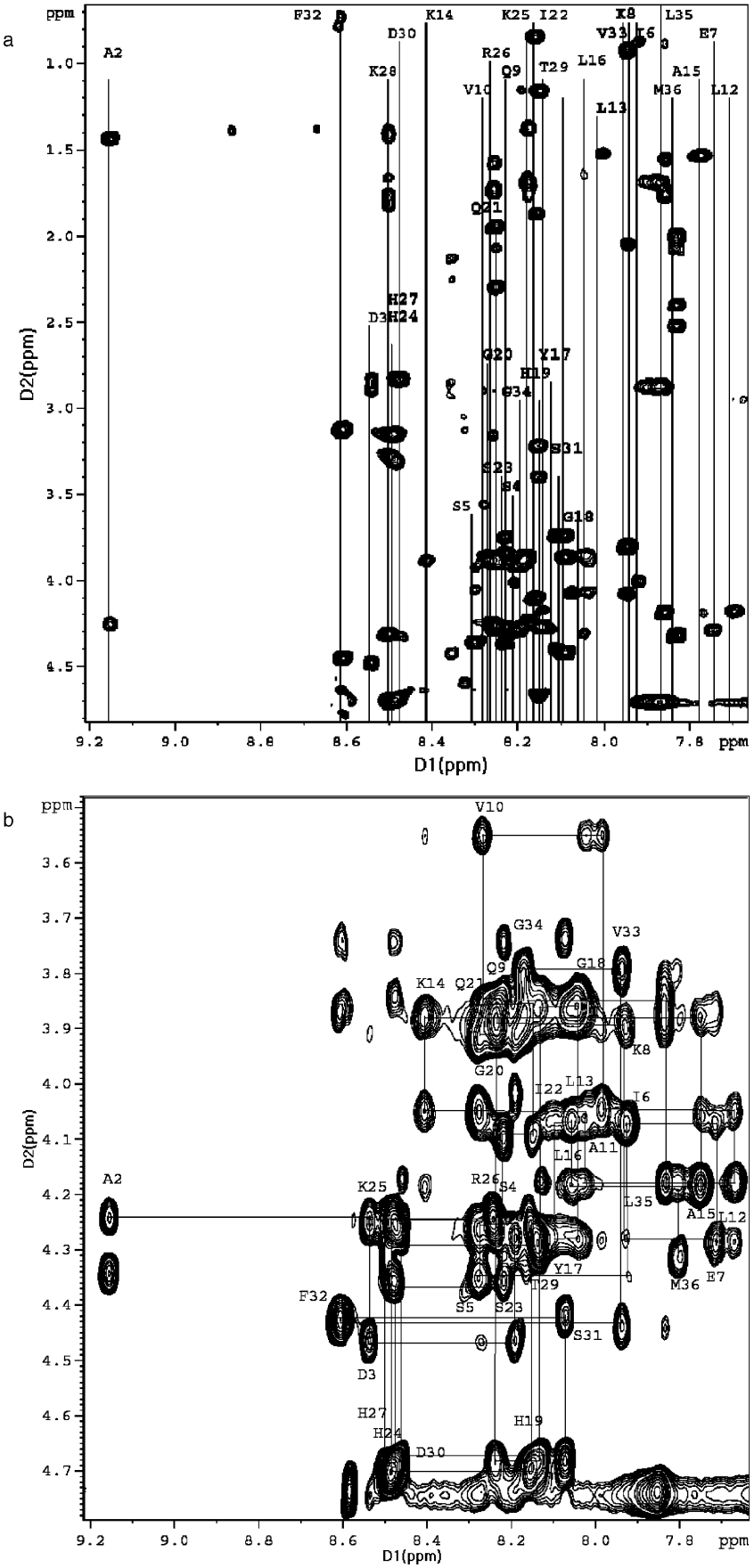

FIGURE 3: (a) Partial 500 MHz ^{1}H NMR 2D TOCSY spectrum (D1 from 9.2 to 7.6 ppm) of 2.4 mM NPK in 146 mM DPC micelles recorded at 305 K and pH 3.5. The spin systems of the amide protons are designated by the amino acid one-letter code, upper-case letters. (b) Partial 500 MHz ^{1}H NMR 2D NOESY (150 ms, mixing time) spectrum (D1 from 9.2 to 7.6 ppm) of 2.4 mM NPK in 146 mM DPC micelles at 305 K. For the sake of clarity, only the intraresidue α-amide cross-peaks are labeled.

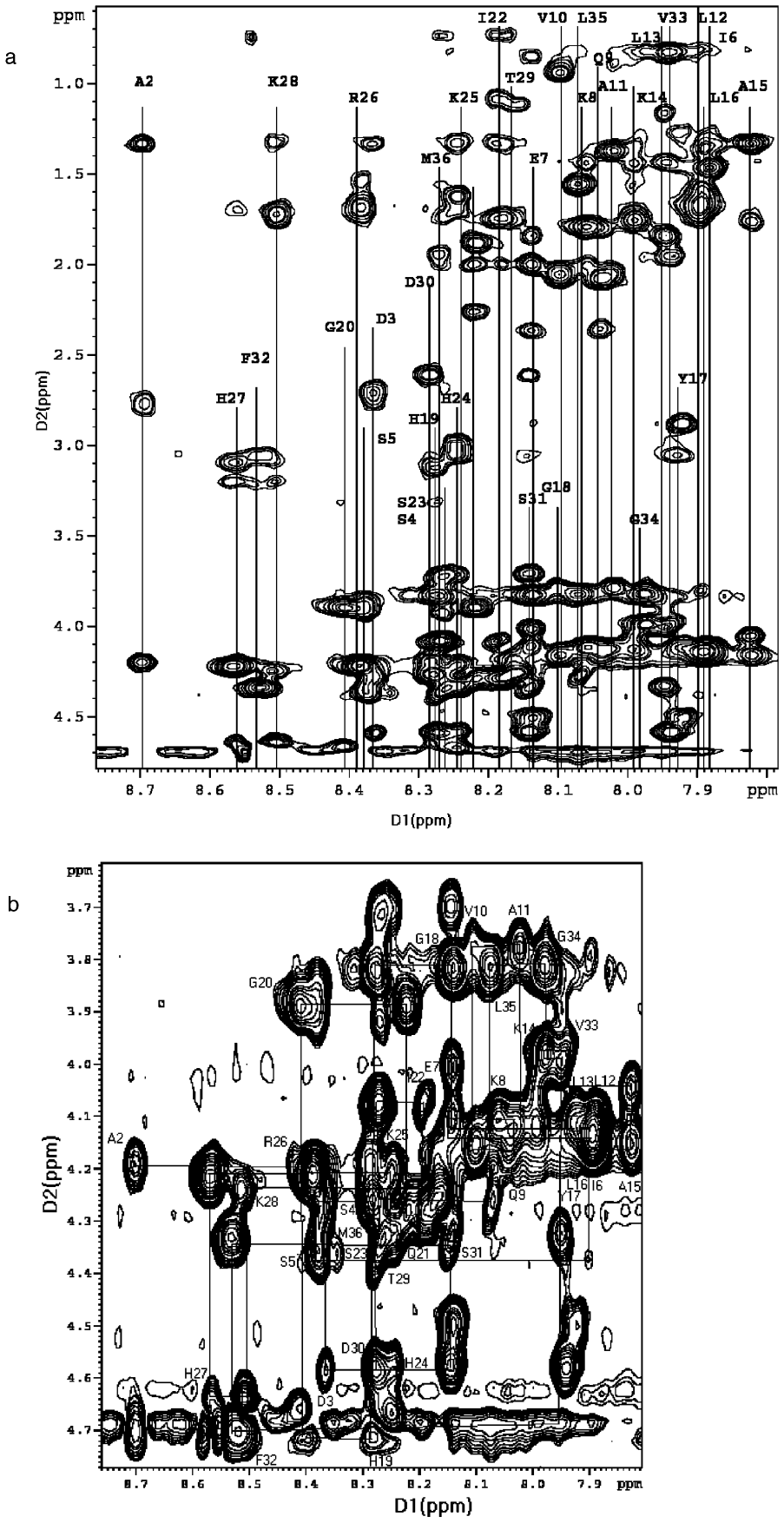

FIGURE 4: (a) Partial 500 MHz ^{1}H NMR 2D TOCSY spectrum (D1 from 8.7 to 7.8 ppm) of 2.4 mM NPK in an aqueous environment (water) at 300 K and pH 3.5. The spin systems of the amide protons are designated by the amino acid one-letter code, upper-case letters. (b) Partial 500 MHz ^{1}H NMR 2D ROESY (150 ms, mixing time) spectrum (D1 from 8.7 to 7.8 ppm) of 2.4 mM NPK in water. For the sake of clarity, only the intraresidue α-amide cross-peaks are labeled.

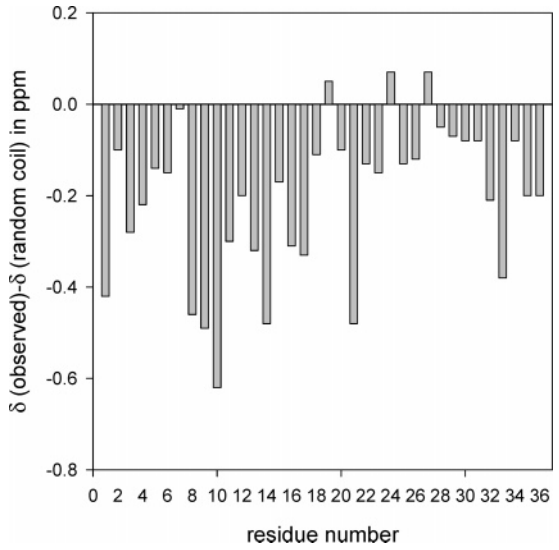

FIGURE 5: Experimental secondary $C_{H\alpha}$ proton chemical shifts for 2.4 mM NPK in the presence of 146 mM DPC micelles, calculated according to random-coil chemical shifts from ref *37*.

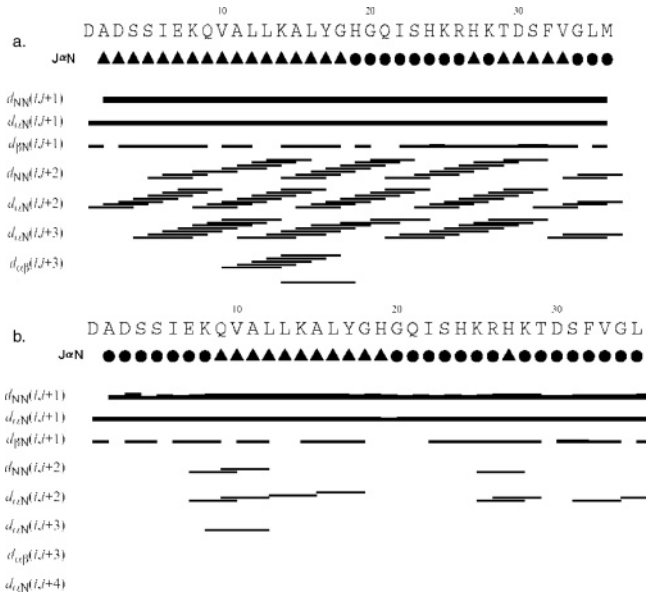

FIGURE 6: Summary of the NOEs that are important to characterize the secondary structure of NPK in the presence of (a) DPC micelles and (b) water. (▲) Coupling constant of 4−5 Hz. (●) Coupling constant of 6 Hz and above.

50 structures were generated, of which 20 conformers with the lowest target function values (i.e., least violations of experimental restraints and van der Waals distances) were chosen for further restrained energy minimization. The superimposition of backbone atoms of 20 structures of NPK (residues 2−18) bound to DPC micelles (Figure 7) shows that the structures are extremely well-defined as judged by low values of the root-mean-square deviation (rmsd) from idealized geometry. The pairwise rmsd calculated for backbone atoms for residues 2−18 for all 20 refined structures is 0.71 ± 0.24 Å. Toward the C terminus, from residues 27 to 33, the pairwise rmsd calculated for backbone atoms is 0.31 ± 0.20 Å.

The Ramachandran plot for all 20 refined structures for the membrane-bound form of NPK (included in the Supporting Information) indicates that the backbone dihedral angles consistently lie in the α region of the plot and are in the favored regions according to the PROCHECK software nomenclature (*48*). The average values of φ and ψ angles for the helix region from 9 to 18 and 27 to 33 are −69.91 ± 1.57 and −21.73 ± 0.92, respectively, and the average values of φ and ψ angles for the turn from 19 to 26 are −75.21 ± 4 and −16 ± 2.92, respectively.

The overall structure of NPK bound to DPC micelles can be described in terms of a clearly defined stretch of α helices (from residues 9 to 18 and 27 to 33) connected by dynamic β turns (from residues 19 to 26). Unwinding or fraying of the helix is observed toward the C-terminal end. The N terminus of the peptide is characterized by a 3_{10} helix or a series of β turns. A side-chain hydrogen bond is observed between Asp1 and Ser4 in all of the 20 structures, which may be important for the stabilization of the N-terminal fold. The helix from residues 9 to 18 forms 2.5 turns and allows the formation of putative hydrogen bonds between the amide HN_i and the carboxyl CO_{i+4} for residues in this region. A similar pattern of hydrogen bonds typical for the α helix is observed in the region from 27 to 33, forming 1.5 turns. When the structures are best-fitted on the backbone residues of the β turn, the local pairwise rmsd of this turn is 0.70 Å. The (i, $i + 3$) hydrogen bond between the CO group of His19 and the NH group of Ile22 resembling classical β turns is found only in 8 of the 20 structures. Similarly, the (i, i + 3) hydrogen bond between the CO group of Ser23 and the NH group of Arg26 is found in 16 of the 20 structures. Although a unique β turn could not be identified, nevertheless, the propensity to adopt a type II′β turn is noticed. The distribution of hydrophobic potentials at the Connolly surface of NPK is presented in Figure 8. The helix from residues 9 to 18 is dominated by hydrophobic residues, with hydrophilic residues occurring at the extremities.

NMR spectroscopy is the method of choice for determining the three-dimensional solution structure of peptides. However, a number of factors such as precision in the estimate of NOE values, use of short interproton distances, approximation of the rational reorientation of the peptide in solution with a single-correlation time model, and the internal mobility of the peptide chain complicate the structure determination.

DISCUSSION

Results from the present study indicate that in an aqueous environment the conformation of NPK is defined by the presence of turn-like elements, with a lack of a definite secondary structure. Both the N-terminal address domain and the C-terminal message domain are folded in a membrane environment. The overall conformational features adopted by NPK in DPC micelles correlate well with that reported for NPK in TFE by Horne et al. (*16*). The presence of a helical core is more pronounced in DPC micelles than in TFE, where in the helical region, it is involved in the Asp3−Gly18 segment. On the contrary, the results reported here show that NPK adopts a helical structure toward the C terminus (from residues 27 to 33) and the whole of the N-terminal region is folded. The presence of series of turns or the 3_{10} helix from residues 2 to 8 can be inferred as intermediates between the folding pathway or unwinding of the helix (from residues 9 to 18). It has been shown that the addition of a structure promoting solvents shifts this equi-

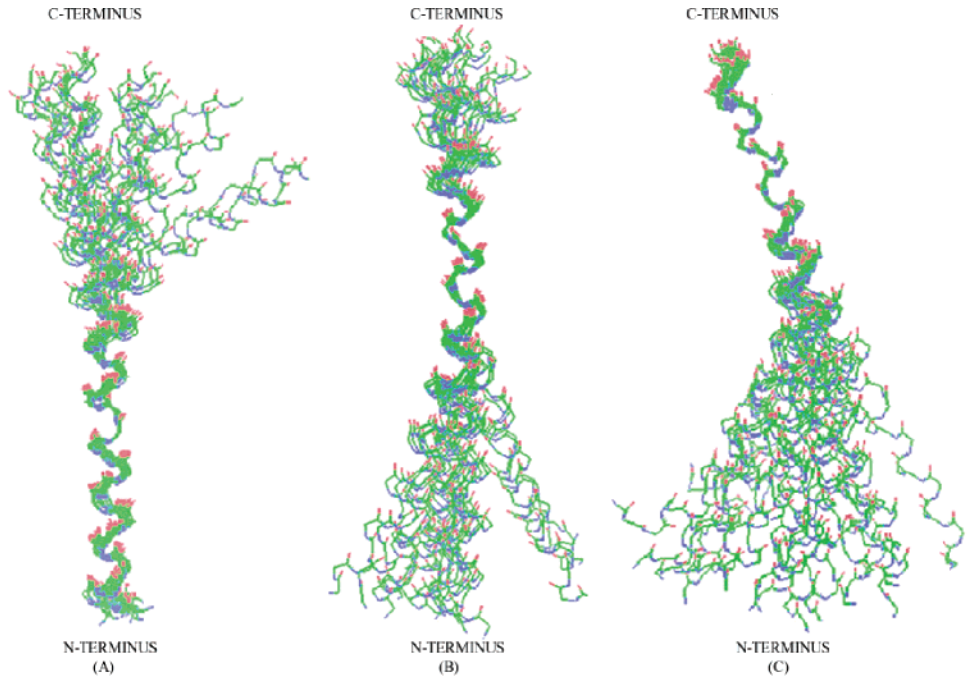

FIGURE 7: Overlay of the 20 structures in the ensemble of NPK in 146 mM DPC micelles. Backbone atoms from (A) Ala 2 to Gly 18, (B) His 19 to Arg 26, and (C) His 27 to Val 33 were superimposed with respect to the restrained minimized average structure.

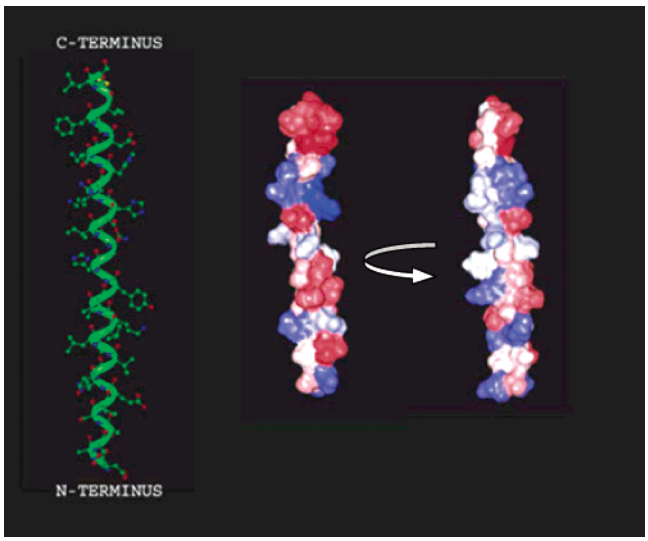

FIGURE 8: Distribution of hydrophobic potentials. (Right) Orthographic view of the hydrophobic potentials at the Connolly surface (radius of 1.4 Å) of NPK. (Left) Schematic representations of the peptide backbone indicating the orientation in the left orthographic view pictures. Hydrophobicity increases from blue to red.

librium toward helix formation (*49*) (extended ↔ turn ↔ 3_{10} helix ↔ α helix). A study on the analysis of the short helices explains that the formation of the β turn might be correlated to the nucleation step for the formation of both α and 3_{10} helices (*50*). The presence of a β turn preceding in the helical core in the C terminus of NPK is consistent with that observed for other NK2 agonists such as NKA, eledoisin, and NPγ in DPC micelles (*20*, *21*, *51*). On the basis of this correlation, it is interesting to note that the conformation adopted by NPK in the presence of DPC micelles presents the structural motif typical of NK2-selective agonists. The presence of an α helix in the C-terminal region is consistent in all NK2 agonists, and the conservation of the primary and secondary structure in the C terminus of NK2 agonists supports the hypothesis that the biological activity and receptor activation are mediated by the C-terminal "message domain" of tachykinins.

Extracellular calcium is essential for the action of tachykinins and has been suggested to impose additional structural constraints on the peptides. The calcium-bound conformation of tachykinins has been suggested to be required for receptor activation (*52*). Our CD studies on calcium titrations with NPK show that the helicity increases with increasing concentrations of calcium. The data suggest that specific constraints may be imposed on the neuropeptide structure on its interaction with calcium, which may have a role in the bioactive conformation of the peptide and its interaction with the receptor. The studies are very preliminary, and more work is needed, however, before the relevance of these observations can be established.

NPK along with NPγ is an N-terminally extended form of NKA. All of the three tachykinins (NKA, NPγ, and NPK) have been shown to be potent NK2 agonists. NPK and NKA are the specific post-translational products of the β preprotachykinin gene, and NPγ is produced by γ preprotachykinin. Despite the common C-terminal message domain in the three tachykinins, NPK has been shown to possess a greater potency at NK2 binding sites than NKA and NPγ. Hence, a comparison of observed conformational features of NPK with NKA and NPγ might be a valuable starting point for the rational design of subsequent structure−activity studies aimed at designing effective agonists or more significantly antagonists for NK2 receptors.

The three-dimensional structures of NKA and NPγ in the membrane environment have been studied previously by our group (*21*, *51*). As shown in Figure 9, the overall fold of NKA is characterized by a helical core in the region from Asp4 to Met10 preceded by a plausible turn toward the N terminus. Similarly, in NPγ, the globular fold is defined as the helical conformation in the central core and the C-terminal region from residues Lys13 to Met21 preceded by a

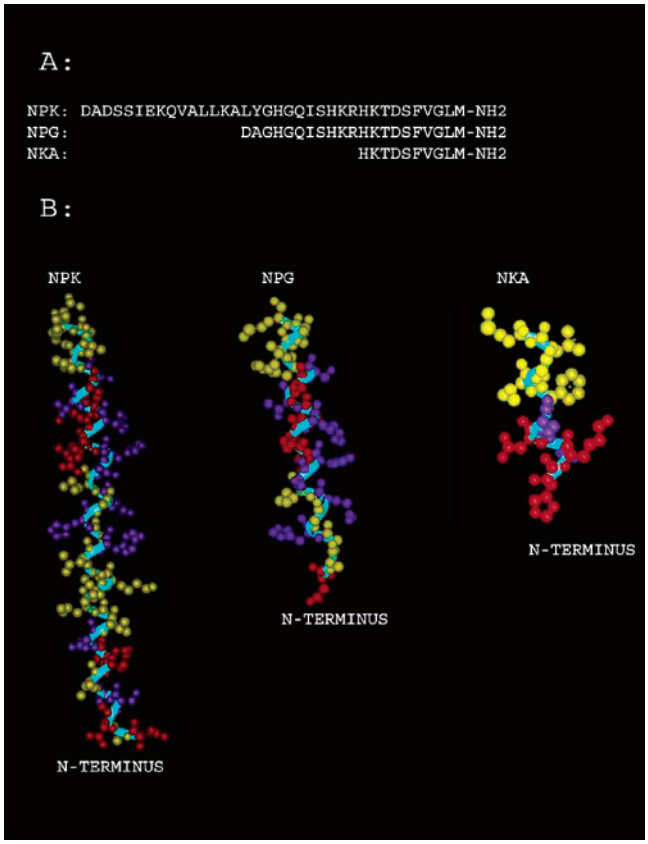

FIGURE 9: Sequence alignment and a graphic representation of the lipid-bound conformation of NPK compared with NPγ and NKA. The peptide backbone is shown as a ribbon tube (blue). Ionic residues are colored red; polar residues are colored purple; and the hydrophobic residues are colored yellow. The helical segment is clearly visible.

turn from His9 to Arg11. The N terminus of NPγ also displays some degree of order and a possible turn structure. Although there are differences in the conformation of the N terminus of NKA, NPγ, and NPK, a similar helical fold is observed in the C terminus of the three peptides.

The region from His27 to Met36 in NPK corresponds to the amino acid sequence of NKA. NPK, NPγ, and NKA are coded by the same gene and are coreleased from the same neurons (*53*). Hence, there is a possibility that NPK and NPγ may act as a precursor of NKA and that the post-translational processing of NPK and NPγ involves an enzymatic processing of the basic β-turn region from residues His24 to Lys28 in NPK and from residues His9 to Lys13 in NPγ. The proteolysis of NPK and NPγ may be regulated in a tissue-specific manner. Krieger and Hook (*54*) determined by identification of proteolytic products through microsequencing and amino acid composition analysis that NPK was cleaved at the Lys-Arg basic residue site. A comparison of the β-turn site comprising these basic residue sites in both NPγ and NPK indicated a very close similarity.

NPK has been shown to have greater potency for the NK2 receptor than NPγ and NKA. This suggests that the N-terminal extension of NKA increases selectivity for the NK2 sites. However, it was proposed by studies on NPγ that the N-terminal elongation of NKA does not appear to influence the binding affinity; rather, it affects the selectivity for NK2 sites (*55*). Further, it was suggested that possession of an acidic residue at position 7 from the C terminus appears to be more critical for NK2 binding (*56*−*58*). It has been proposed that the N-terminal domains of tachykinins affect the desensitization of the receptor and that the N-terminal extension of NKA results in a maximal receptor desensitization (*58*). This suggests that the N-terminal region of NPK that extends beyond NKA containing the C terminus contains information required for maximal receptor desensitization (*59*). Dependent upon the structure of the ligand, an agonist-occupied receptor may adopt distinct conformations that are functionally active with respect to G-protein activation but show different susceptibility to kinases involved in desensitization. Possible explanations for these differential effects of N-terminal extension of tachykinin sequences include the effects of the N-terminal peptide domain on the C-terminal peptide conformation or the N-terminal domain that may make additional contacts with the NK2 receptor. Thus, the amino-terminal domains of these peptides may have a dual role, one in stabilizing a conformation leading to receptor kinase activation and desensitization and the other in conferring selectivity for the NK2 receptor (*58*). Alternatively, the amino-terminal portion of the N-terminally extended peptides may lock or modulate the binding conformation of the C-terminal domain by intramolecular interactions, thus reducing the overall flexibility of the peptide.

In conclusion, it can be seen from Figure 9 that the C terminus presents a hydrophobic upper half comprising Phe32, Val33, Gly34, Leu35, and Met36 residues and a hydrophilic middle region extending from Ser31 to His19, which also includes a stretch of basic residues comprising His24−Lys28. Paired basic residues of Lys25 and Arg26 are proposed to be the site for proteolytic cleavage of NKA and from its precursor NPK. We propose that the hydrophobic C terminus of NPK gets inserted into the transmembrane region of the receptor, whereas the N terminus possibly interacts with the extracellular loops and helps in positioning the C terminus within the transmembrane region. Phe32, Leu35, and Met36 of the peptide possibly form the anchoring points in the NK2 receptor, contributing a major portion of the binding energy. Further, the α helix (residues 27−33) itself and also its particular orientation, which is provided by the N terminus, are required to provide the conformational prerequisites of residues important for receptor binding. The sequence alignment of NKA, NPγ, and NPK and the comparison of their structures lead us to hypothesize that a common procedure of receptor binding exists. In fact, the single residue responsible for the binding to the membrane, the overall backbone structure of the C-terminal address domain, is conserved, and the greater potency of NPK at the NK2 receptors can be attributed to the folded N-terminal domain.

Because the structural features of the peptide ligand have been determined in isolation, there could be conformational alterations to the structure upon the interaction with the receptor. However, these structural features, which seem to be essential for the biological activity, will probably be maintained until NPK approaches its receptor. Nevertheless, this could be a valuable starting point for the design of NPK analogues to be used as pharmacological tools, particularly useful, because classical structure−activity relationship data are still not available for this peptide.

ACKNOWLEDGMENT

The staff of the National 500 and 600 MHz NMR Facility at Sophisticated Instruments Facility, Indian Institute of Science, Bangalore and Tata Institute of Fundamental Research, Mumbai, as well as discussions with Professor G. Govil, Professor K. V. R. Chary, and Dr. S. Raghothama are gratefully acknowledged. Dr. Indu R. Chandrashekar is thanked for her initial help in this work. One of the authors (A. D.) acknowledges the financial support in the form of a Senior Research Fellowship from the Council of Scientific and Industrial Research, India. This work is supported by a grant from the Department of Science and Technology, Government of India.

SUPPORTING INFORMATION AVAILABLE

Table 3, proton NMR assignments of NPK in the presence of DPC micelles; Table 4, proton NMR assignments of NPK in the presence of water; Supporting Figure, Ramachandran plot of the final 50 structures calculated (in DPC micelles). This material is available free of charge via the Internet at http://pubs.acs.org.

REFERENCES

1. Tatemoto, K., Lundberg, J. M., Jornvall, H., and Mutt, V. (1985) Neuropeptide K: Isolation, structure, and biological activities of a novel brain tachykinin, *Biochem. Biophys. Res. Commun. 128*, 947−953.
2. Decarie, A., and Couture, R. (1992) Characterization of the peripheral action of neuropeptide K on the rat cardiovascular system, *Eur. J. Pharmacol. 213*, 125−131.
3. Arai, H., and Emson, P. C. (1986) Regional distribution of neuropeptide K and other tachykinins (neurokinin A, neurokinin B, and substance P) in rat central nervous system, *Brain Res. 399*, 240−249.
4. Diez-Guerra, F. J., Richardson, P. J., and Emson, P. C. (1988) Subcellular distribution of mammalian tachykinins in rat basal ganglia, *J. Neurochem. 50*, 440−450.
5. Takeda, Y., and Krause, J. E. (1989) Neuropeptide K potently stimulates salivary gland secretion and potentiates substance P-induced salivation, *Proc. Natl. Acad. Sci. U.S.A. 86*, 392−396.
6. Prat, A., Hassessian, H., and Couture, R (1993) Neuropeptide K potently stimulates the hydrolysis of phosphatidylinositol in the rat spinal cord, *Neurosci. Lett. 159*, 95−98.
7. Martling, C. R., Theodorsson-Norheim, E., Norheim, I., and Lundberg, J. M. (1987) Bronchocontrictor and hypotensive effects in relation to pharmacokinetics of tachykinins in the guinea-pig evidence for extraneuronal cleavage of neuropeptide K to neurokinin A, *Naunyn−Schmiedeberg's Arch. Pharmacol. 336*, 183−189.
8. Nakanishi, S. (1991) Mammalian tachykinin receptors, *Annu. Rev. Neurosci. 14*, 123−136.
9. Masu, Y., Nakayama, K., Tamaki, H., Harada, M., Kuno, Y., and Nakanishi, S. (1987) cDNA cloning of bovine substance-K receptor through oocyte expression system, *Nature 329*, 836−838.
10. Hanley, M. R., and Jackson, T. (1987) Substance K receptor: Return of magnificent seven, *Nature 329*, 766−767.
11. Beaujouan, J. C., Saffroy, M., Petitet, F., Torrens, Y., and Glowinski, J. (1988) Neuropeptide K, scyliorhinin I, and scyliorhinin II: New tools in the tachykinin receptor field, *Eur. J. Pharmacol. 151*, 353−354.
12. Convert, O., Ploux, O., Lavielle, S., Cotrat, M., and Chassaing, G. (1988) Analysis of tachykinin-binding site interactions using NMR and energy calculation data of potent cyclic analogues of subtsnace P, *Biochem. Bhiophys. Acta 954*, 287−302.
13. Convert, O., Duplaa, H., Levielle, S., and Chassiang, G. (1991) Influence of the replacement of amino acid by its D-enantiomer in the sequence of substance P; conformational analysis by NMR and energy calculations, *Neuropeptides 19*, 259−270.
14. Seelig, A. (1992) Interaction of a substance P agonist and of substance P antagonists with lipid membranes: A thermodynamic analysis, *Biochemistry 31*, 2897−2904.
15. Ananthanarayanan, V. S., and Orlicky, S. (1992) Interaction of substance P and its N- and C-terminal fragments with Ca^{2+}: Implications for hormone action, *Biopolymers 32*, 1765−1773.
16. Horne, J., Sadek, M., and Craik, D. J. (1993) Determination of solution structure of neuropeptide K by high-resolution nuclear magnetic resonance spectroscopy, *Biochemistry 32*, 7406−7412.
17. Cowsik, S. M., Luke, C., and Ruterjans, H. (1997) Lipid-induced conformation of substance P, *J. Biomol. Struct. Dyn. 15*, 27−36.
18. Whitehead, T. L., McNair, S. D., Hadden, C. E., Young, J. K., and Hicks, R. P. (1998) Membrane-induced secondary structures of neuropeptides: A comparison of solution conformations adopted agonists and antagonists of the mammalian tachykinin NK1 receptor, *J. Med. Chem. 41*, 1497−1506.
19. Grace, C. R., Lynn, A. M., and Cowsik, S. M. (2001) Lipid induced conformation of tachykinin peptide kassinin, *J. Biomol. Struct. Dyn. 18*, 611−625.
20. Grace, C. R., Chandrashekar, I. R., and Cowsik, S. M. (2003) Solution structure of the tachykinin peptide eledoisin, *Biophys. J. 84*, 655−664.
21. Chandrashekar, I. R., and Cowsik, S. M. (2003) Three-dimensional structure of the mammalian tachykinin peptide neurokinin A bound to lipid micelles, *Biophys. J. 85*, 1−10.
22. Mantha, A., Chandrashekar, I. R., and Cowsik, S. M. (2004) Three-dimensional structure of the mammalian tachykinin peptide neurokinin B bound to lipid micelles, *J. Biomol. Struct. Dyn. 22*, 137−147.
23. Dike, A., and Cowsik, S. M. (2005) Membrane induced structure of Scyliorhinin I: A dual NK1/NK2 agonist, *Biophys. J. 88*, 3592−3600.
24. Schwyzer, R. (1995) 100 years lock and key concept: Are peptide keys shaped and guided to their receptors by the target cell membrane? *Biopolymers 37*, 5−16, review.
25. White, S. H., and Wimley, W. C. (1994) Peptides in lipid bilayers: Structural and thermodynamic basis for partitioning and folding, *Curr. Opin. Struct. Biol. 4*, 79−86.
26. Sargent, D. F., and Schwyzer, R. (1986). Membrane lipid phase as catalyst for peptide−receptor interactions, *Proc. Natl. Acad. Sci. U.S.A. 83*, 5774−5778.
27. Schwyzer, R. (1995). In search of the "bioactive conformation"—Is it induced by the target cell membrane? *J. Mol. Recognit. 8*, 3−8.
28. Moroder, L., Romano, R., Guba, W., Mierke, D. F., Kessler, H., Delporte, C., Winand, J., and Christophe, J. (1993) New evidence for a membrane-bound pathway in hormone receptor binding, *Biochemistry 32*, 13551−13559.
29. Lerch, M., Mayrhofer, M., and Zerbe, O. (2004) Structural similarities of Micelle-bound peptide YY (PYY) and neuropeptide Y (NPY) are related to their affinity profiles at the Y receptors, *J. Mol. Biol. 339*, 1153−1168.
30. Maurer, T., and Ruterjans, H. (1994) Solution structure of seminal plasmin in the presence of micelles, *Eur. J. Biochem. 220*, 111−116.
31. Rizo, J., Blanco, F. J., Kobe, B., Bruch, M. D., and Gierasch, L. M. (1993) Conformational behavior of *Escherichia coli* OmpA signal peptides in membrane mimetic environments, *Biochemistry 32*, 4881−4894.
32. Inooka, H., Ohtaki, T., Kithara, O., Ikegami, T., Endo, S., Kitada, C., Ogi, K., Onda, H., Fujino, M., and Shirkawa, M. (2001). Conformation of ligand bound to its G-protein coupled receptor, *Nat. Struct. Biol. 8*, 161−165.
33. Braun, W., Wider, G., Lee, K. H., and Wüthrich, K. (1983) Conformation of glucagons on lipid water interface by ^{1}H-nuclear magnetic resonance, *J. Mol. Biol. 169*, 921−948.
34. McDonnell, P. A., and Opella, S. J. (1993) Effect of detergent concentration on multidimensional solution NMR spectra of membrane proteins in micelles, *J. Magn. Reson., Ser. B 102*, 120−125.
35. Opella, S. J. (1997) NMR and membrane proteins, *Nat. Struct. Biol. NMR Supplement 10*, 845−848.
36. Kallick, D. A., Tessmer, M. R., Watts, C. R., and Li, C. (1995) Use of dodecyl phosphocholine micelles in solution NMR, *J. Magn. Reson., Ser. B 109*, 60−65.
37. Wüthrich, K. (1986) *NMR of Proteins and Nucleic Acids*, J. Wiley and Sons, New York.

38. Güntert, P., Mumenthaler, C., and Wüthrich, K. (1997) Torsion angle dynamics for NMR structure calculation with the new program DYANA, *J. Mol. Biol. 273*, 283−298.
39. Sreerama, N., and Woody, R. W. (2000) Estimation of protein secondary structure from CD spectra: Comparison of CONTIN, SELCON, and CDSSTR methods with an expanded reference set, *Anal. Biochem. 282*, 252−260.
40. Bruch, M. D., Dhingra, M. M., and Gierasch, L. M. (1991) Side chain−backbone hydrogen bonding contributes to helix stability in peptides derived from an α-helical region of carboxypeptidase A, *Proteins: Struct., Funct., Genet. 10*, 130−139.
41. Marion, D., and Wüthrich, K. (1983) Application of phase sensitive two-dimensional correlated spectroscopy (COSY) for measurement of ^{1}H−^{1}H spin−spin coupling constants in protein, *Biochem. Biophys. Res. Comun. 113*, 967−974.
42. Pardi, A., Billeter, M., and Wüthrich, K. (1984) Calibration of the angular dependence of the amide proton-C α proton coupling constants, $^3J_{HN\alpha}$, in a globular protein. Use of $^3J_{HN\alpha}$ for identification of helical secondary structure, *J. Mol. Biol. 180*, 741−751.
43. Holzworth, G., and Doty, P. (1965) The ultraviolet circular dichroism of polypeptide, *J. Am. Chem. Soc. 87*, 218−228.
44. Alder, A. J., Greenfield, N. J., and Fasman, G. D. (1973) Circular dichroism and optical rotatory dispersion of proteins and polypeptides, *Methods Enzymol. 27*, 675−735.
45. Chang, T. C., Wu, C.-S. C., and Yang. J. T. (1978) Circular dichroic analysis of protein conformation: Inclusion of the β-turns, *Anal. Biochem. 91*, 13−31.
46. Wishart, D. S., Sykes, B. D., and Richards, F. M. (1992) The chemical shift index: A fast and simple method for the assignment of protein secondary structure through NMR spectroscopy, *Biochemistry 31*, 647−1651.
47. Wüthrich, K., Billeter, M., and Braun, W. (1984) Polypeptide secondary structure determination by nuclear magnetic resonance observation of short proton−proton distances, *J. Mol. Biol. 180*, 715−740.
48. Laskowski, R. A., MacArthur. M. W., Moss. D. S., and Thornton, J. M. (1993). PROCHECK: A program to check the stereochemical quality of protein structures, *J. Appl. Crystallogr. 26*, 283−291.
49. Osterhout, J. J., Jr., Baldwin, R. I., York, E. J., Stewart, J. M., Dyson, H. J., and Wright, P. E. (1989) ^{1}H NMR study of the solution conformation of an analogue of the C-peptide of ribonuclease A, *Biochemistry 28*, 7059−7064.
50. Pal, L., Chakrabarti, P., and Basu, G. (2003) Sequence and structure patterns in proteins from an analysis of the shortest helices: Implications for helix nucleation, *J. Mol. Biol. 326*, 273−291.
51. Chandrashekar, I. R., Dike, A., and Cowsik, S. M. (2004) Membrane induced structure of mammalian neuropeptide γ, *J. Struct. Biol. 148*, 315−325.
52. Ananthanarayanan, V. S., and Orlicky, S. (1992) Interaction of substance P and its N- and C-terminal fragments with Ca^{2+}: Implications for harmone action, *Biopolymers 32*, 1765−1773.
53. Krause, J. E., Chirgwin, J. M., Carter, M. S., Xu, Z. S., and Hershey, A. D. (1987) Three rat preprotachykinin mRNAs encode the neuropeptides substance P and neurokinin A, *Proc, Natl. Acad. Sci. U.S.A. 84*, 881−885.
54. Krieger, T. J., and Hook, V. Y. (1992) Purification and characterization of a cathepsin D protease from bovine chromaffin granules, *Biochemistry 31*, 4223−4231.
55. Badgery-Parker, T., Lovas, S., Conlon, J. M., and Burcher, E. (1993) Receptor binding profile of neuropeptide γ and its fragments: Comparison with the nonmammalian peptides carassin and ranakinin at three mammalian tachykinin receptors, *Peptides 14*, 771−775.
56. Severini, C., Salvadori, S., Guerrini, R., Falconnieri-Erspamer, G., Mignogna, G., and Erspamer, V. (2000) Parallel bioassay of 39 tachykinins on 11 smooth muscle preparations. Structure and receptor selectivity/affinity relationship, *Peptides 21*, 1587−1595.
57. Matuszek, M. A., Comis, A., and Burcher, E. (1999). Binding and functional potency of neurokinin A analogues in the rat fundus: A structure−activity study, *Pharmacology 58*, 227−235.
58. Nemeth, K., and Chollet, A. (1995) A single mutation of the neurokinin-2 (NK2) receptor prevents agonist-induced desensitization, *J. Biol. Chem. 270*, 27601−27605.
59. Vigna, S. R. (2003) The role of the amino-terminal domain of tachykinins in neurokinin-1 receptor signaling and desensitization, *Neuropeptides 37*, 30−35.

BI052287O